DEVELOMENT OF AN AI-ENHANCED CONCEPTUAL AIRCRAFT DESIGN SYNERGY FOR THE RAPID PREDICTION OF FUTURE DRONE CONCEPTS

Mars Burke and Alvin Gatto,[1]

[1]*Mechanical and Aerospace Engineering, Brunel University London, Uxbridge, UK*
Mars.burke@brunel.ac.uk, brunel.ac.uk

Abstract: The use of Unmanned Aerial Vehicles(UAVs) has expanded rapidly over the last decade. These systems have an almost limitless scope of application with resupply, surveillance, monitoring, and logistics representing but a few. Having such a wide scope, a means to rapidly, efficiently and accurately develop new designs fit-for-purpose would offer a significant advantage to developers given their inherent need to maximize potential within a competitive marketplace. This work attempts to leverage the capabilities of Artificial Intelligence(AI) for this purpose through the development of a functional AI model aimed primarily at enhancing initial conceptual design metric prediction using limited inputs and/or datasets. Overall, this synergy shows the potential to improve this process significantly through facilitating faster, more cost-effective design cycle iterations allowing ultimately more effective and efficient decision making.

1. Introduction

Artificial intelligence/Machine Learning (AI/ML) has become a transformative tool within aircraft design by addressing the growing complexity of systems and the need for optimization across multiple disciplines. From aerodynamics and propulsion to structural integrity and systems integration, AI techniques have proven instrumental in enabling faster, more efficient, and innovative designs.

The integration of AI into aerodynamic optimization is one area of particular note widely considered. At their core, these techniques are often used to enhance more traditional aerodynamic design techniques which tend to be much more computationally or labor intensive (Computational Fluid Dynamics (CFD), wind tunnel testing) and limit the scope of exploration within the design space. In this way, the integration of AI techniques have since emerged as a viable practical alternative, reducing computational and experimental costs while maintaining fidelity. Some techniques such as the use of Genetic Algorithms (GAs) have also emerged as powerful tools for navigating such complex design spaces, enabling a multi-objective optimization formulation by simultaneously considering dissimilar variables like aerodynamic performance, structural weight, and fuel efficiency. Haryanto et al. (2014) demonstrated the use of such techniques to optimize airfoil configurations for maximum lift-to-drag ratios allowing for significant performance gains while reducing computational demand. Similarly, Duvigneau and Visonneau (2004) combined GAs with Artificial Neural Networks (ANNs) to create hybrid optimization frameworks leveraging the exploratory capabilities of GAs with the predictive efficiency of ANNs.

Wei et al. (2024) also used ANNs when introducing DeepGeo, a neural-network-based framework that simultaneously optimized shape and mesh deformation within the design space. This model was found to simplify the parameterization process, allowing for faster convergence to optimal aerodynamic configurations. They also highlighted the potential of AI to directly handle high-dimensional geometric and aerodynamic variables making it a valuable tool for complex design scenarios. Similarly, Mandia et al. (2024) demonstrated the use of multi-fidelity modelling in optimizing winglet configurations. By combining high and low-resolution datasets, their approach was considered to have achieved a balance between computational efficiency and predictive accuracy; both critical factors in early aircraft design stages. Another study by Ghoreyshi et al. (2024) further explored reduced-order modelling techniques such as Proper Orthogonal Decomposition (POD), undertaking efforts to simplify the often very complex flow dynamics into manageable computational problems, further accelerating the design process. In similar ways, Osco et al. (2021) also demonstrated that use of Convolutional Neural networks(CNNs) could be used to identify flow patterns and predict aerodynamic coefficients, significantly reducing the need for extensive computational simulations.

Predictive modelling is another domain where AI has made significant contributions, particularly in evaluating aircraft performance metrics. Predictive tools developed using AI can facilitate the rapid assessment of multiple design candidates, enabling more informed decision-making during conceptual and preliminary design phases. Trani et al. (2004) applied ANNs to model fuel consumption across different flight phases, achieving high predictive accuracy. These models could allow designers to evaluate the fuel efficiency of various configurations without relying on costly physical tests or simulations. Similarly, Tong (2020) employed AI/ML algorithms to predict thrust-specific fuel consumption (TSFC) and engine core size, providing a reliable framework for optimizing propulsion systems.

The use of reinforcement learning in aircraft design has also shown considerable promise. Unlike traditional optimization methods, reinforcement learning adapts dynamically to feedback, allowing for iterative refinement of designs. Zhang et al. (2024) applied deep reinforcement learning to wing optimization, demonstrating its ability to evolve configurations that achieve superior aerodynamic efficiency compared to conventional approaches. By simulating complex flow environments, these algorithms were used to refine design parameters to optimize performance metrics such as lift, drag, and stability characteristics. This adaptability has shown significant promise and makes reinforcement learning particularly valuable for addressing non-linear, multi-objective challenges inherent in most aircraft design problems.

In addition to optimization, AI has been instrumental in addressing challenges related to structural design and materials. Similarly, the design of lightweight yet strong aircraft structures also involves balancing competing objectives such as load-bearing capacity, fatigue resistance, and manufacturability. Azizi Oroumieh et al. (2013) employed fuzzy logic and neural networks to model key structural parameters for light business jets. Machine learning algorithms, including support vector machines and decision trees, have also been used to model and predict material properties based on experimental and computational data(Sun & Wang, 2019). Another subset of AI known as Transfer learning, which leverages pre-trained models for new tasks, has also been particularly effective in this area, enabling researchers to apply insights from existing datasets to new material systems (Dong & Ai, 2023).

The role of AI within the design space also extends to encompass integrated system design. Modern aircraft comprise highly interconnected subsystems, including propulsion units, avionics, and environmental controls. Coordinating these subsystems to achieve optimal performance necessitates sophisticated optimization frameworks. Garriga et al. (2019) developed an AI-enabled multi-disciplinary platform that evaluated aircraft configurations at varying fidelity levels. This system was deployed primarily to advance electrification of primary flight control systems and landing gear to align with the industry's push toward sustainable aviation. Multi-objective optimization frameworks that incorporate AI techniques have also been successfully applied to balance subsystem interactions (Haryanto et al., 2014) as well as reinforcement learning to manage trade-offs between conflicting design goals, such as maximizing thrust while minimizing noise pollution (Zhang et al., 2024).

Autonomous systems design has also emerged as a critical area of research within AI-driven aircraft design. UAVs are increasingly incorporating autonomous design features, requiring robust decision-making algorithms capable of handling dynamic environments. Within this theme, Reinforcement learning and fuzzy logic systems have been applied to optimize control strategies for autonomous flight (Ali, 1990). These methods enable adaptive behaviour, such as real-time trajectory adjustments and mission planning, enhancing the reliability and efficiency of autonomous systems. Explainable AI techniques, like SHAP and LIME, are also being integrated into these systems to provide transparency in decision-making processes which is considered an important precursor for adequately addressing regulatory and safety concerns (Ramrao et al., 2023; Sun & Wang, 2019).

Data-driven approaches have also further expanded the scope of AI in aircraft design. The vast amounts of data generated during design and testing phases, including telemetry, wind tunnel experiments, and CFD simulations, provide a rich foundation for machine learning models. Gradient boosting and ensemble methods have been employed to analyse these datasets, extracting actionable insights that inform design decisions (Dong & Ai, 2023). Transfer learning within this framework has also enabled the application of insights from one domain to another, such as adapting UAV design principles to commercial aviation applications (Sun et al., 2019). Transformer architectures, with their ability to process sequential data, have also been explored for applications such as dynamic load prediction and flutter analysis (Li et al., 2023).

Despite its successes, the use of AI in aircraft design faces several challenges. One significant issue is the interpretability of AI models, particularly in safety-critical applications. Black-box models, while potentially accurate, often lack the transparency needed for regulatory approval and operational trust (Ali, 1990; Brunton et al., 2021). Some techniques seek to offer solutions to these issues by providing interpretable explanations for model predictions, however, their integration into complex design workflows continues to remain ongoing.

Data availability and quality are further challenges, particularly in early-stage design with high-fidelity data required for training machine learning models often very scarce and/or expensive to obtain. Synthetic data generation and data augmentation techniques are gaining some traction though via several techniques and solutions enabling researchers to simulate realistic datasets that enhance model robustness (Duvigneau & Visonneau, 2004; Mandia et al., 2024). Computational efficiency also remains a significant concern, especially for real-time applications. While surrogate models and reduced-order methods have mitigated some of these challenges, scaling AI frameworks to handle the growing complexity of aircraft systems still requires much more consideration(Haryanto et al., 2014; Kou & Zhang, 2023).

This work aims to explore and leverage the use of AI in developing a functional relationship for the prediction of initial conceptual design metrics to maximum rated engine power for bespoke UAV platforms. To that end, this work describes; 1) the formulation, manipulation, characterisation, and rational behind the generation of the baseline dataset; 2) use of the dataset for the deployment and training of the chosen AI architecture for future adoption within a more streamlined and efficient conceptual design process; 3) subsequent efforts at both

verification and validation, and lastly; 4) a basic assessment of the capabilities of the AI model for this purpose as well as identification of the best optimised AI architecture within this application framework.

2. External database development and characterization

Having reviewed the current state-of-the-art in AI/ML methods within the context of initial conceptual design practices, the basic Feed-Forward, Neural Network(FFNN) was selected as the main architecture for subsequent use as this type offered a simple, but still potentially accurate solution for the intended application. In order to initially evaluate this choice, an external database including more than 200 individual UAV platforms of varying configuration, type, and application was formulated. Rotary wing configurations were excluded with the sole focus centred on traditional fixed-wing variants. Overall, one of the primary aims of the database was to seek out and include as many relevant examples over as varied and diverse range as possible to ensure maximum applicability and representation to any future developed models. The scope therefore was deliberately selected to encompass from the nano/micro sector(wing span < 0.3 m) through to the large UAV category(~ 30 m) to evaluate if AI/ML use is both appropriate and worthwhile. All information collated for the database was obtained from both online and reference text sources(Janes, 2024) with online information typically derived directly from the manufacturer. After completion, the final constructed database included UAV platforms dating back to the late 1950's through to present day. Countries of origin were taken from examples all over the world with entry into service including operational status both active and retired. Also included were examples which are within active development and/or production. Included UAVs cited were produced by several different individual companies with specified Ranges(R) extending from ~ 2 km to 10000 km, Endurance(E) from ~ 15 min to 3600 min, maximum rated engine power(P) between ~ 9W to 1.2MW, wing span(S) from ~ 0.15m to 26m and maximum operational altitudes(Alt) up to ~16km above ground level. Propulsion layouts included both tractor and pusher propellers operating both electric and internal combustion engine sources. Many were catapult launched variants (i.e electric, hydraulic, pneumatic), with others possessing either conventional, parachute, airbag, parafoil recovery systems, deep-stall, automated belly landers, or skids for landing. Both high tail configurations, low tail with a high wing, and low wing inclusive are included. A select few had an offensive/attack capability/mission set with some armament deployment functionality, with others tasked within solely an Intelligence, Surveillance and/or Reconnaissance (ISR) remit.

2.1 Basic trends and correlations

Before deploying higher order methods, cursory examination of the general trends existing within the dataset was considered worthwhile in order to establish any obvious characteristics and relationships. This analysis would also be beneficial, at the very least anecdotally, in establishing if the presented comparisons meet with general qualitative expectations. For this purpose, Figures 1-6 show various performance and baseline metric comparisons representative of those that could be used early within an initial conceptual design phase as a result of customer drone requirements and needs. Included are Range, Endurance, maximum altitude and speed(V), all compared against maximum rated engine power normalised by M(Maximum Take-Off Mass), along with wing span(S) verses overall platform length. These metrics represented the most cited parameters from the various sources consulted during external dataset assembly with other metrics much more difficult to obtain in the required quantities for widespread or reliable use/characterisation.

On first inspection, significant data scatter within most figures is characteristic, making trend and correlation identification somewhat challenging. This is particularly evident within Figure 1 highlighting Range vs P/M. Overall, results tend to suggest for the varied array of platforms included, a wide bandwidth of Ranges exist across all P/M ratios presented with the possible exception of highest P/M values. In this case, appearance seems to favour lower range expectations(< 400km). This appears somewhat logical at first glance as higher P/M tends to infer higher energy consumption, and possibly, less efficient flight characteristics. Another feature of potential interest within this data is the apparent wide scope of achievable ranges($0 < R < 1800$km) for $P/M < 300$ W/kg suggesting this region perhaps represents a somewhat wider scope of applications within this particular dataset. It should also be remembered however that the number of datapoints remains relatively low and a more extensive dataset is needed to confirm such assertations. The overall indicative trend seems to suggest lower range capabilities with increasing P/M.

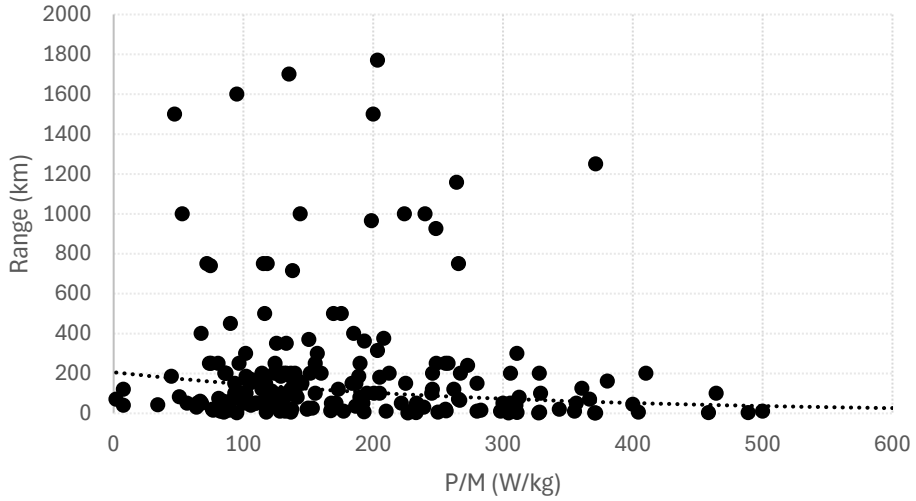

Figure 1. Range vs P/M ratio

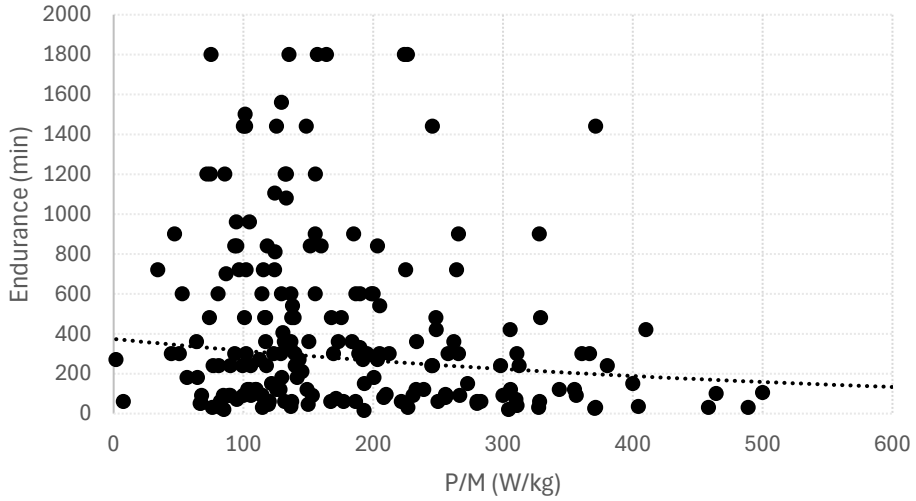

Figure 2. Endurance vs P/M ratio

Figure 2 highlighting the relationship between Endurance and P/M shows similar attributes. In this instance, scatter again remains significant below P/M < 300 W/kg, with this region indicating achievable Endurance limits extending from just minutes to many hours. These results also suggest, in general agreement with Figure 1, that Endurance is inversely correlated(loosely) to P/M with lower Endurance at higher P/M.

The variation of Altitude with P/M continues the overarching trend of observed data scatter(Figure 3). In this case, notwithstanding some data outliers, Altitude also appears to be loosely correlated with the inverse of P/M ratio. A seemingly more obvious trend is evident in Figure 4 showing the relationship between maximum level speed and P/M. In this case, and while significant data scatter continues to remain, achievable maximum speed appears generally correlated with increasing P/M. This result would also tend to agree with expectations given higher P/M platforms would normally be designed with higher wing loading for the target application.

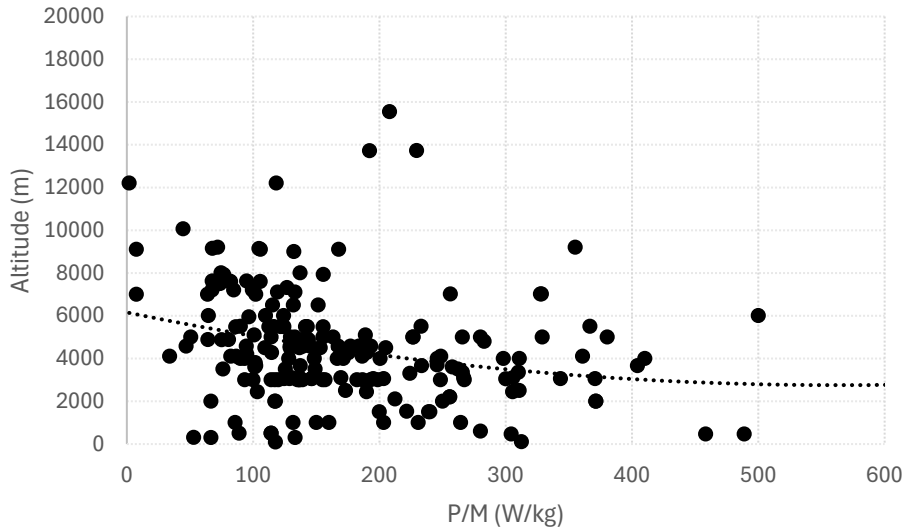

Figure 3. Altitude vs P/M ratio

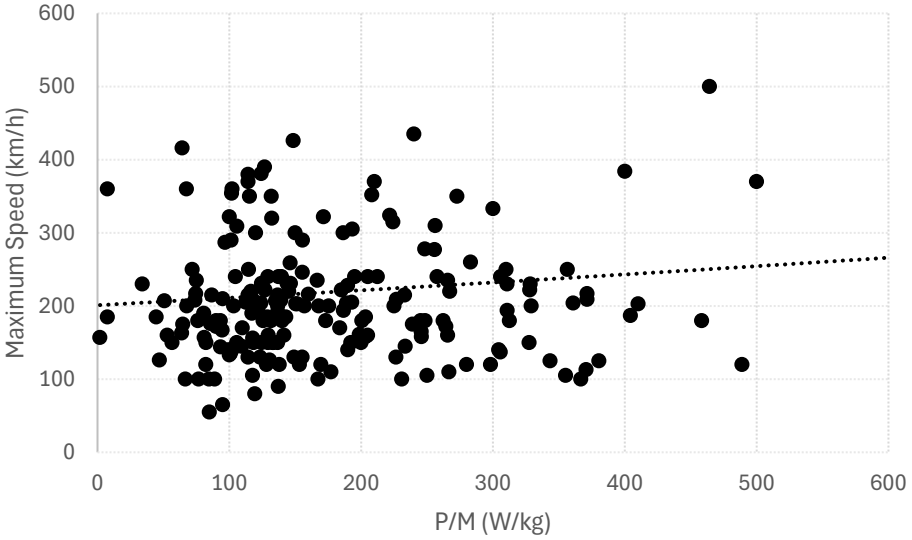

Figure 4. Maximum speed vs P/M ratio

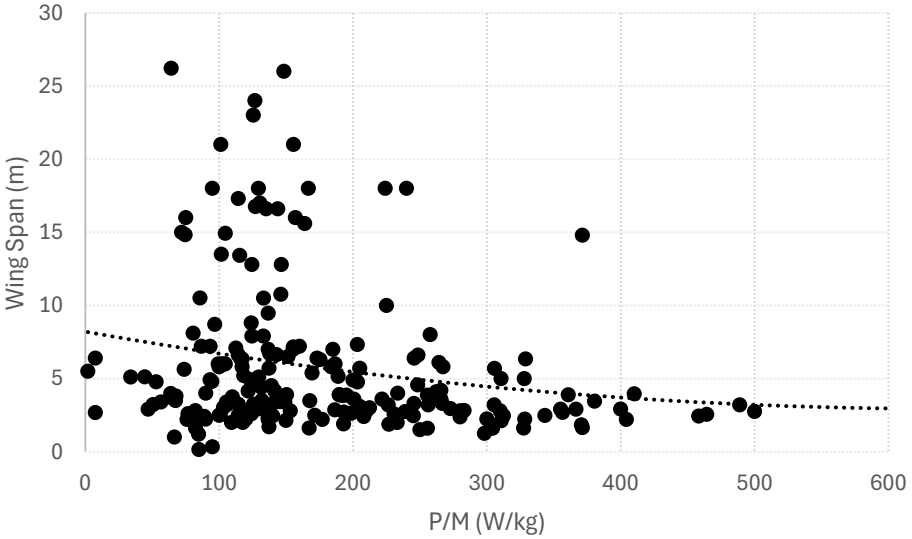

Figure 5. Wing span vs P/M ratio

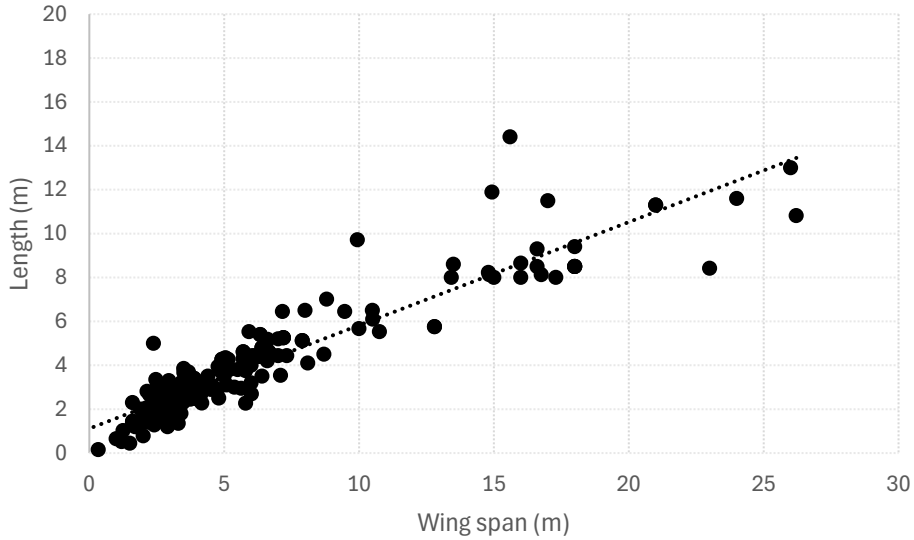

Figure 6. Overall length vs Wing span

Figure 5 further supports this premise providing additional evidence that smaller wing span configurations correlate with higher P/M ratio. This relationship again appears just as variable as shown above at lower values of P/M, but for higher P/M, appear much less so. A much more obvious correlation is finally highlighted in Figure 6 with overall platform length against wing span. This is remarkably well defined within the chosen dataset with platform length well correlated to approximately half that of specified wing span.

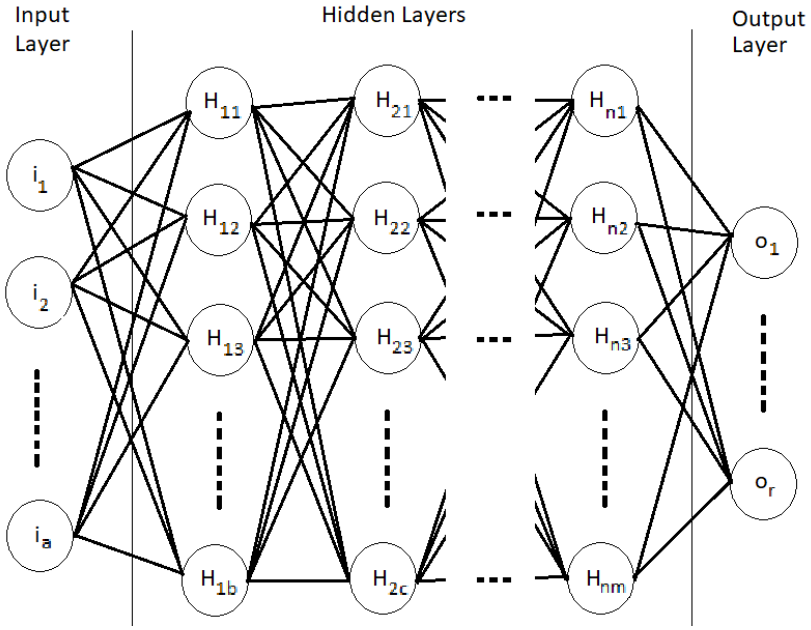

Figure 7. Generalised ANN structure

3. External database AI model architecture

At its core, the FFNN is a type of Artificial Neural Network(ANN) that attempts to effectively map a relationship between a set of input parameters to target outputs modelled on the behaviour of the human brain (Khanna,1996). Figure 7 shows a generalised structure composed of an input layer(i) of depth a, n hidden layers, each with its own individual depth(in this case b, c, and for the nth layer, m), and a final output layer, o, of depth r. Each hidden neuron is characterised as a summation node with individual weights from each preceding neuron(along with a bias) fed forward through a non-linear activation function to subsequent layers. Error assessments are then made and weights modified thereafter proceeding the next subsequent cycle. This process is repeated continuously using

the complete dataset(or epoch, E) until acceptable or set fidelity metrics are achieved. Typically, the dataset is pre-split into training/validation/test sets (i.e 70/15/15 split); the former used to learn data characteristics; the next or validation set used to assess model performance on as yet unseen data points and to tune hyperparameters; with the latter, to test and assess the final trained and fine-tuned validated model against another independent set of data.

Various accuracy metrics can be used to assess network performance each with its own advantages and disadvantages. Ultimately, this choice depends largely on either the goals of the modelling and/or dataset character. In this instance, a combination of Mean Squared Error(MSE) and R-squared metrics were used to assess overall model capabilities and fitness for purpose.

MSE remains one of the most common metrics for assessing predictive accuracy within regression applications. Overall, MSE represents the average squared difference between the predicted($\hat{y}_i$) and target(y_i) values over N samples(Eq. 1). The aim of using this model is to minimize MSE with better indicative performance achieved with smaller MSE. R-squared uses a Sum of Squares of Errors (SSE) to the Total Sum of Squares (SST) relationship (Eq. 2) to indicate how closely two datasets relate to one another. Overall, R-squared has a maximum of one for perfectly fit data with values below that (including less than zero) suggesting the model does not, to varying degrees, fully represent the data characteristics.

$$MSE = \frac{1}{N}\sum_{i=1}^{N}(y_i - \hat{y}_i)^2 \quad \text{(Eq. 1)}$$

$$R^2 = 1 - \frac{SSE}{SST} \quad \text{(Eq. 2)}$$

3.1 External database training, validation and testing

To train and validate the selected AI model architecture, an iterative process was developed and applied to encompass a wide array of hidden layer and neuron number per layer. Various parameters including the influence of dropout(DR), batch size(BS), learning rate(LR) and E were considered, albeit for the latter, most used an imposed limit of 1000 as a trade-off between computational resources and achievable model performance. Within this process, the number of hidden layers(N) was varied from one to ten manually with each layer containing up to a maximum of 64 neurons each. Given the scope of the investigation and to minimise training time scales, the number of neurons in each hidden layer was configured to be identical per layer as the indexing process took place each time. For the first AI/ML model developed based on the external Database, five inputs(M, S, R, E, and V) and one output(P) were used to construct the model.

The training and validation methodology adopted deployed supervised learning on proportionally split, normalised, randomly shuffled, data segments in each case. A further segment processed in a similar way was also split for test use; this set representing a further independent, never before been seen, number of example cases. Prior shuffling of the data ensured captured, unrelated patterns within data that were order-based were minimised. This can be an important consideration particularly when dealing with relatively small, wide-ranging datasets spanning multiple orders of magnitude. In this case, shuffling randomly rearranged the data order prior to each epoch ensuring no data order visibility during each epoch existed promoting generalization. During training, the FFNN sought to minimise prediction errors by iteratively adjusting weights and biases using the Adam optimisation algorithm guided by the MSE loss function. All hidden layers used the ReLU activation function in order to capture the inherent complex, non-linear relationships within the dataset with the single node output layer deploying a linear activation function to provide predicted values. Unless otherwise indicated, dropout rates of 0, 10%, 20%, and 30%, where a randomly selected number of neurons during training were deactivated were considered to enhance generalisation and limit overfitting, were also used with every hidden layer. Throughout this process, the Gradient Descent algorithm was adopted to minimize the loss function via iterative parameter model weight and bias updating.

The final performance evaluation and validation of the FFNN against the externally-derived data subset used MSE and R-squared metrics to assess fidelity. Considered in unison, these metrics were considered most appropriate to provide insights into the model capabilities in terms of accuracy and generalization.

3.2 External database AI model assesment

The basic methodology adopted in developing the FFNN was notionally one of exploratory investigation and interactive result interpretation with subsequent development/feedback. As a first step in this process, the initial model architecture was set to an upper limit of ten hidden layers, with up to 64 neurons per layer, and 1000 epochs without dropout. Table 1 highlights the first five ranked lowest MSE training and test loss and best R-squared(highest) from the analysis. On first inspection, and as would be expected, the level of training and test

loss is reduced with increase in training and test R-squared as the model better reflects the characteristics of the data. It also appears that both hidden-layer count and number of neurons per layer is relatively large (HL ~ 6-8 and N ~ 19-23) to achieve these results under these conditions. Interestingly batch size appears largely uncorrelated and much less sensitive. For these cases also it can be seen that the R-squared training values outperform the R-squared test results significantly due, most likely, to the disproportionate dataset sizes used for each. Nevertheless, the results seem to suggest somewhat encouraging ultimate performance, with best R-squared training and test metrics being 0.9978 and 0.9131 respectively. These values indicate that this model architecture can represent and predict the test data adequately. In this case, the best parameters were HL=8, N=23, BS=80, DR=0, LR = 0.001 and E=1000. As might also be expected, higher fidelity predictive capabilities appear to coincide with increasing HL count with changing DR having no material effect under these circumstances for this particular dataset. Figures 8-10 also highlight results for R-squared(test) against various other parameters.

Rank	Hidden Layers	Neurons per Layer	Batch Size	R-squared (Training)	R-squared (Test)	Mean Squared Error (Training)	Mean Squared Error (Test)
1	8	23	80	0.9978	0.9131	3510000	1480000000
2	6	23	30	0.9933	0.8156	10900000	3130000000
3	8	19	90	0.9938	0.8146	10000000	3150000000
4	2	11	20	0.9841	0.8133	25900000	3170000000
5	2	26	80	0.9901	0.8058	16000000	3300000000

Table 1. Top 5 FNN Model Architecture results for DR=0, LR = 0.001 and E=1000.

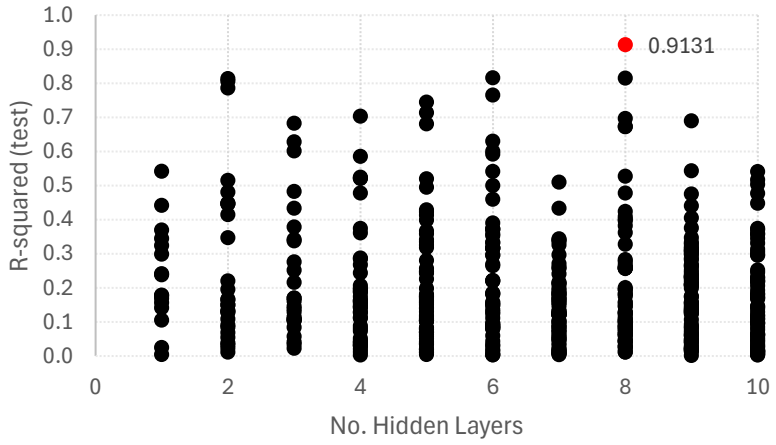

Figure 8. Influence of Hidden Layer No. with DR=0, 10<BS<100, LR=0.001, 2<N<64 and E=1000.

To further explore the capabilities of the FFNN, this process was deployed a second time with E increased to 10000 for the same LR (LR=0.001). In this case, completion of the full test matrix used a total running cluster time of approximately 3 weeks. Table 2 highlights these results. As can be seen, the application of the higher number of epochs appears to have improved the R-squared(test) metric from 0.9131 to 0.9541 with a corresponding decrease in HL, N, and BS to 2, 4, and 30 from 8, 23, and 80 respectively. Of note also is the reduction in the R-squared(training) from 0.9978 to 0.9784 corresponding to this improvement in MSE(test) relative to E=1000(Table 1). These findings seems to suggest that with larger E, less complex AI model architectures may be more characteristic and provide for a better solution. Similarly, Figures 11-13 show some of these characteristics.

Having considered these initial explorations at LR=0.001, a full exploratory investigation was subsequently undertaken encompassing a more comprehensive parameter space investigation to include $1 < HL < 10$, $1 < N < 64$, $10 < BS < 100$, $0.001 < LR < 1$, and $100 < E < 10000$. Table 3 shows a summary of the best results obtained.

Overall, increasing LR to LR = 0.01 is shown to degrade achievable model fidelity at the lowest E, before producing a model with generally improved model performance at E = 1000. Whilst hidden layer number indicates relatively consistency at this higher LR, optimal N appears to nearly double for optimal results. A further increase to LR = 0.1 shows an additional degradation in model performance at lowest E compared to the previous LR considered, whilst remaining generally in line at E = 1000. Further increase to LR = 1 extends this trend further with model performance being the lowest observed within the complete optimisation space considered. Ultimately, the final model chosen as the best compromise is highlighted in Table 3 and utilised the following parameters; HL = 8, N = 45, BS = 50, LR = 0.01 and E = 1000.

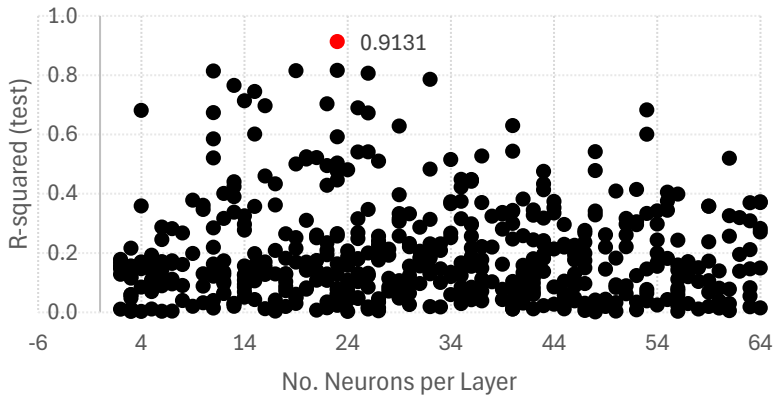

Figure 9. Influence of No. Neurons per Layer with DR=0, 10<BS<100, LR=0.001, 1<HL<11 and E=1000.

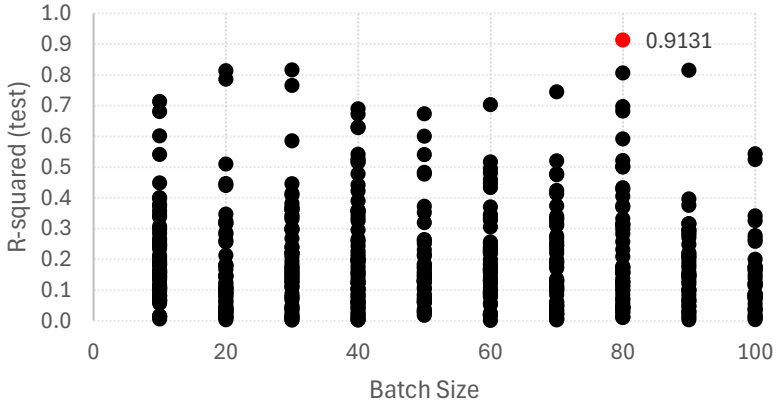

Figure 10. Influence of Batch Size with DR=0, 10<BS<100, LR=0.001, 1<HL<11, 2<N<64 and E=1000.

Rank	Hidden Layers	Neurons per Layer	Batch Size	R-squared (Training)	R-squared (Test)	Mean Squared Error (Training)	Mean Squared Error (Test)
1	2	4	30	0.9784	0.9541	35100000	780000000
2	2	13	10	0.998	0.8581	3320000	2410000000
3	1	21	90	0.9947	0.8282	8650000	2920000000
4	7	6	50	0.9969	0.7773	5080000	3780000000
5	1	40	10	0.9741	0.7482	42100000	4280000000

Table 2. Top 5 FNN Model Architecture results for DR=0, LR = 0.001 and E=10000.

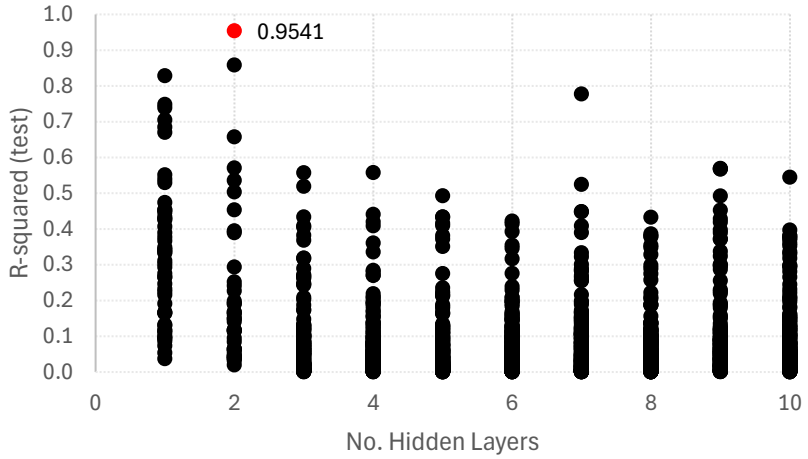

Figure 11. Influence of Hidden Layer No. with DR=0, 10<BS<100, LR=0.001, 2<N<64 and E=10000.

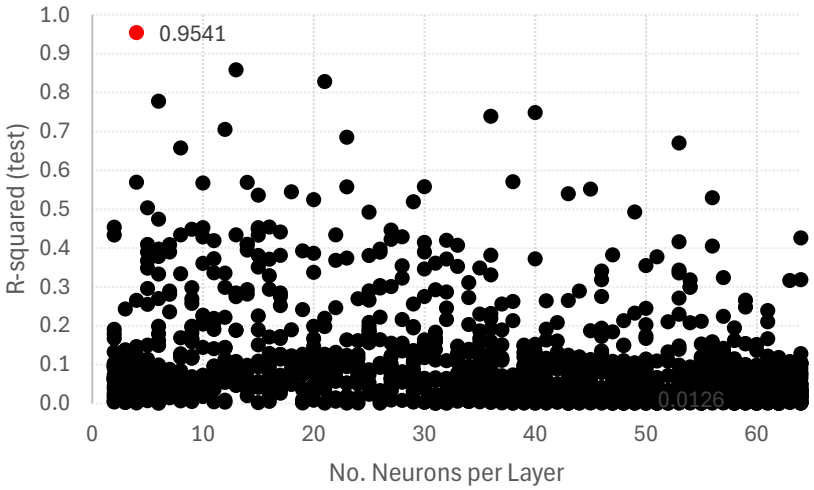

Figure 12. Influence of No. Neurons per Layer with DR=0, 10<BS<100, LR=0.001, 1<HL<11 and E=10000.

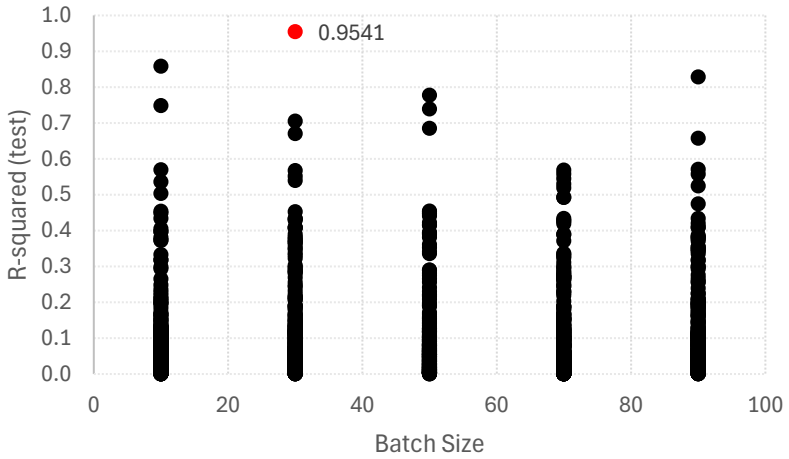

Figure 13. Influence of Batch Size with DR=0, LR=0.001, 1<HL<11, 2<N<64 and E=10000.

Hidden Layers	Neurons per Layer	Batch Size	Learning Rate	Epochs	R-squared (Training)	R-squared (Test)	Mean Squared Error (Training)	Mean Squared Error (Test)
6	57	10	0.001	100	0.9947	0.8874	110000000	298000000
8	23	80	0.001	1000	0.9978	0.9131	3510000	1480000000
2	4	30	0.001	10000	0.9784	0.9541	35100000	780000000
2	44	10	0.01	100	0.9497	0.8787	1020000000	494000000
8	45	50	0.01	1000	0.9888	0.933	22800000	273000000
9	30	30	0.01	10000	0.7087	0.913	6040000000	229000000
5	17	30	0.1	100	0.7455	0.888	5270000000	296000000
2	46	90	0.1	1000	0.9965	0.8365	71600000	432000000
2	26	70	0.1	10000	0.7475	0.8723	5230000000	338000000
2[1]	46	10	1	100	0.5072	0.7166	10300000000	749000000
1	30	30	1	1000	0.4434	0.7932	11500000000	547000000
4	47	90	1	10000	0.1151	0.1835	18300000000	216000000

Table 3. Summary of best FNN Model Architecture results for various hyperparameter combinations.

4 Conclusion

Application of a AI/ML feed-forward neural network to rapidly predict basic initial conceptual design characteristics of UAV platforms has been presented. A database of externally sourced past and present UAV platforms(>200) was used to predict maximum engine performance from five input variables, maximum take-off mass, wing span, range, endurance, and maximum level fight speed. The final optimised architecture chosen after investigating various parameter configurations was 8 hidden layers, with 45 neurons per layer over 1000 epochs. This model showed generally very good correlation between actual supplied data and model predictions (R-squared(test) = 0.933). Once developed, the model showed significant potential to leveraged the near-instantaneous capabilities of ML/AI to benefit the initial conceptual design phase of any future bespoke UAV platforms.

References

1. Haryanto, I., Utomo, M. S. K. T. S., Sinaga, N., Rosalia, C. A., & Putra, A. P., Optimization of maximum lift to drag ratio on airfoil design based on artificial neural network utilizing genetic algorithm. *Applied Mechanics and Materials*, **2014**, 493, 123-128. https://doi.org/10.4028/www.scientific.net/AMM.493.1

2. Duvigneau, R., & Visonneau, M., Hybrid Genetic Algorithms and Artificial Neural Networks for Complex Design Optimization in CFD. *International Journal for Numerical Methods in Fluids*, **2004**, 44(11), 1257-1278. https://doi.org/10.1002/fld.741

3. Wei, Z., Yang, A., Li, J., Bauerheim, M., Liem, R. P., & Fua, P., DeepGeo: Deep Geometric Mapping for Automated and Effective Parameterization in Aerodynamic Shape Optimization. *AIAA AVIATION FORUM AND ASCEND 2024*. https://doi.org/10.2514/6.2024-3839, **2024**.

4. Mandia, V., Sharma, V., Chandra, Y., Kumar, G. and Singh, R.K., Optimizing Winglet Cant Angle for Enhanced Aircraft Wing Performance Using CFD Simulation and Hybrid ANN-GA. *Int J Numer Meth Fluids*. **2024**, https://doi.org/10.1002/fld.5341

[1]These results were obtained with a dropout rate of 10%. For all other results shown, dropout rate was zero.

5. Ghoreyshi, M., Jirásek, A., & Cummings, R. M., Computational approximation of nonlinear unsteady aerodynamics using an aerodynamic model hierarchy. *Aerospace Science and Technology*, **2013**, 28(1), 133–144, https://doi.org/10.1016/j.ast.2012.10.009

6. Osco, L. P., Marcato Junior, J., Marques Ramos, A. P., de Castro Jorge, L. A., Fatholahi, S. N., de Andrade Silva, J., Matsubara, E. T., Pistori, H., Gonçalves, W. N., & Li, J., A review on deep learning in UAV remote sensing. *International Journal of Applied Earth Observation and Geoinformation*, **2021**, 102, 102456. https://doi.org/10.1016/j.jag.2021.102456

7. Trani, A., Wing-Ho, F., Schilling, G., Baik, H., & Seshadri, A., A neural network model to estimate aircraft fuel consumption. *AIAA 4th Aviation Technology, Integration and Operations (ATIO) Forum, Chicago, Illinois*, 20–22 September **2004**. https://doi.org/10.2514/6.2004-6401

8. Tong, M. T., Machine learning-based predictive analytics for aircraft engine conceptual design (NASA/TM-20205007448), National Aeronautics and Space Administration, Glenn Research Center, **2020**.

9. Zhang, Z., Ao, Y., Li, S., & Gu, G. X., An adaptive machine learning-based optimization method in the aerodynamic analysis of a finite wing under various cruise conditions. *Theoretical and Applied Mechanics Letters*, **2024**, 14, 100489,

10. Azizi Oroumieh, M. A., Malaek, S. M. B., Ashrafizaadeh, M., & Taheri, S. M., Aircraft design cycle time reduction using artificial intelligence. *Aerospace Science and Technology*, **2013**, 26(1), 244-258, https://doi.org/10.1016/j.ast.2012.03.013

11. Sun, W., & Wang, L., A Review of Artificial Neural Network Surrogate Modeling in Aerodynamic Design. *Aerospace Science and Technology*, **2019**, 93, Article 105332, https://doi.org/10.1016/j.ast.2019.105332.

12. Garcia Garriga, A., Mainini, L., & Ponnusamy, S. S., A machine learning-enabled multi-fidelity platform for the integrated design of aircraft systems. *Journal of Mechanical Design*, **2019**, 141(12), 121405, https://doi.org/10.1115/1.4044401

13. Ali, M., Intelligent systems in aerospace. *The Knowledge Engineering Review*, **1990**, 5(3), 147-166. https://doi.org/10.1017/S0269888900005385

14. Ramrao, A., Subhash, T., & Pandurang, S., AI-Driven Predictive Maintenance for Aerospace Engines. *Journal of Propulsion Technology*, **2023**, 19(2), 150-168. https://doi.org/10.1016/j.jproptech.2023.005202.

15. Dong, Y., & Ai, J., Research on estimating method of fuel and emissions using neural networks in LTO cycle for preliminary aircraft design. *28th International Congress of the Aeronautical Sciences (ICAS), Shanghai, China,* **2012.**

16. Brunton, S. L., Kutz, J. N., Manohar, K., Aravkin, A. Y., Morgansen, K., Klemisch, J., Goebel, N., Buttrick, J., Poskin, J., Blom-Schieber, A., Hogan, T. A., & McDonald, D., Data-driven aerospace engineering: Reframing the industry with machine learning. *AIAA Journal*, **2021**, 59(7), 2820-2847. https://doi.org/10.2514/1.J060131

17. Kou, J., & Zhang, W.. Data-driven modelling for unsteady aerodynamics and aeroelasticity. *Progress in Aerospace Sciences,* **2021**,125, 100725.

18. Khanna, T., “Foundations of Neural Networks.”, New York., Addison-Wesley., **1996**.

19. Jane's All the World’s Aircraft: Unmanned Yearbook, *2024/2025 Edition, Jane's Group*, ISBN9780710634474.